In Vivo Oxygen Uptake into the Human Cornea

Sho C. Takatori,[1] *Percy Lazon de la Jara,*[2,3] *Brien Holden,*[2,3] *Klaus Ehrmann,*[2] *Arthur Ho,*[2,3] *and Clayton J. Radke*[1,4]

Purpose. We provide a new procedure to quantify in situ corneal oxygen uptake using the micropolarographic Clark electrode.

Methods. Traditionally, upon placing a membrane-covered Clark microelectrode onto a human cornea, the resulting polarographic signal is interpreted as the oxygen partial pressure at the anterior corneal surface. However, the Clark electrode operates at a limiting current. Hence, oxygen flux is directly detected rather than partial pressure. We corrected this misunderstanding and devised a new analysis to quantify oxygen uptake into the cornea. The proposed analysis is applied to new polarographic data for 10 human subjects during open-eye oxygen uptake.

Results. Average open-eye corneal oxygen uptake over 10 subjects is approximately 11 μL/(cm^2 h), approximately five times larger than the average reported by researchers who invoke the original mathematical analysis. Application of the classical interpretation scheme to our experimental data also garners uptake values that are approximately a factor of three to five times smaller than those obtained with our new procedure.

Conclusions. The classical procedure originally developed by Fatt and colleagues misinterprets the behavior of the Clark microelectrode. We corrected the analysis of the in situ polarographic technique to provide a simple yet rigorous procedure for analyzing both previous data in the literature and those newly obtained. Our proposed interpretation scheme thus provides a reliable tool for in vivo assessment of corneal oxygen uptake. (*Invest Ophthalmol Vis Sci.* 2012;53:6331–6337) DOI:10.1167/iovs.12-10059

Atmospheric oxygen supply to the anterior cornea supports aerobic metabolism and suppresses hypoxic swelling.[1–3] In addition to edema, detrimental effects of oxygen deficiency in corneal physiology include hypoesthesia, acidosis, epithelial microcysts, stromal and epithelial thinning, and increased endothelial polymegathism.[4–6] Consequently, specifying the oxygen demand of the human cornea has received major attention and some debate.[7–27] With few exceptions,[28–31] most of these efforts focus on mathematical modeling.[1–3,10,27,32–38] In some cases, however, theoretical prediction may not faithfully represent clinical response.

Currently, the most often-used experimental method for ascertaining atmospheric oxygen flux into the human cornea is that of Fatt et al.[39–41] employing micropolarography with a Clark oxygen electrode.[42,43] The polarographic technique is well established and extensively used to assess in vivo oxygen uptake into the human cornea both with and without contact lens wear.[7,28,29,39–41,44–63] For use on the human eye, the Clark microelectrode is covered with a thin protective polymer membrane and is gently placed either directly on the cornea or on a worn contact lens. The resulting transient electrode signal is reported as the oxygen partial pressure at the anterior corneal or lens surface.[7,28,29,39–63] The initial linear slope of a semilogarithmic graph of measured partial pressure versus time is ascertained and is related to the steady flux of oxygen or oxygen uptake into the cornea prior to microelectrode placement.[40,51,52,54,55,59,63] Unfortunately, we find that the classical interpretation scheme is flawed.

Materials and Methods

A Clark electrochemical cell detects the electrical current arising from the reduction of aqueous oxygen at the cathode surface,[42,43]

$$O_2 + 2H_2O + 4e^- \rightarrow 4OH^- \qquad (1)$$

Provided that the applied voltage is sufficient, the current at the limiting plateau value is independent of voltage.[28,42,43,45,64] At limiting current, the concentration of oxygen at the electrode surface is practically zero.[64–67] Thus, oxygen diffuses through the membrane toward the cathode. Fatt and colleagues assumed that oxygen initially in the protective membrane diffused only into the cornea with no oxygen flux into the cathode.[39–41] For this reason, the standard procedure to analyze the measured oxygen-tension decline is invalid and cannot reliably yield oxygen uptake into the cornea.

We correct the analysis of the Clark electrode measurement to provide a reliable assessment of in vivo anterior oxygen uptake by the human cornea. Transient oxygen partial pressures rigorously follow exponential decline only at later times. Long-time data are analyzed with a physically correct model of the polarographic-tension data to assess the average metabolic oxygen kinetic rate constant in the cornea. Once the kinetic rate is quantified, calculation of oxygen uptake is straightforward. Newly measured micropolarographic data are presented for 10 human subjects under open-eye conditions. Analysis of the clinical data with the proposed interpretation scheme allows a simple and consistent evaluation of human-corneal oxygen uptake.

From the [1]Department of Chemical and Biomolecular Engineering and the [4]Vision Science Group, University of California, Berkeley, California; the [2]Brien Holden Vision Research Institute, Sydney, NSW, Australia; and the [3]School of Optometry & Vision Science, University of New South Wales, Sydney, NSW, Australia.

Submitted for publication April 19, 2012; revised June 21, 2012; accepted July 9, 2012.

Disclosure: **S.C. Takatori**, None; **P. Lazon de la Jara**, Australian Government Cooperative Research Centre Program (F), Brien Holden Vision Institute (F, E); **B. Holden**, Australian Government Cooperative Research Centre Program (F), Brien Holden Vision Institute (F, E); **K. Ehrmann**, Australian Government Cooperative Research Centre Program (F), Brien Holden Vision Institute (F, E); **A. Ho**, Australian Government Cooperative Research Centre Program (F), Brien Holden Vision Institute (F, E); **C.J. Radke**, None

Corresponding author: Clayton J. Radke, Department of Chemical and Biomolecular Engineering, University of California, 101E Gilman, Berkeley, CA 94720-1462; radke@berkeley.edu.

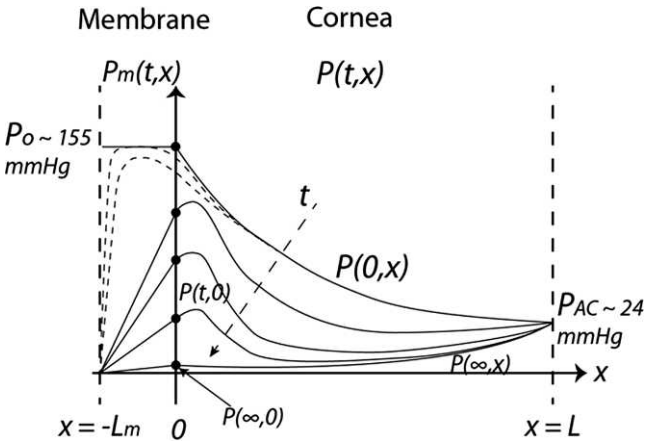

Figure 1. Schematic of oxygen partial-pressure profiles upon placing a microelectrode onto the cornea. *Solid curves* represent illustrative transient oxygen-tension profiles in the covering membrane, $P_m(t,x)$, of thickness, L_m, and in the cornea, $P(t,x)$, of thickness, L. The *dashed line with an arrow* denotes progression of time. Initially, the corneal oxygen supply is from the environment giving a tension profile of $P(0,x)$. *Dashed curves* represent the early time profiles before a pseudosteady state is established in the membrane. *Filled circles* along the membrane/anterior cornea interface at $x = 0$ represent the measured oxygen tension.

Oxygen Transport

Figure 1 shows expected transient oxygen partial-pressure profiles upon placing the Clark electrode probe onto the cornea. We adopted a one-dimensional analysis, although with a 20-μm thick membrane covering a 30-μm diameter cathode, some radial supply of oxygen is anticipated.[68] We also neglected axial diffusive resistance of the thin electrolyte film (ca. 3 μm) between the cathode and the covering membrane and that of the thin tear film (ca. 1–2 μm) between the covering membrane and the cornea. In Figure 1, $x = -L_m$ corresponds to the membrane/cathode interface, $x = 0$ locates the membrane/anterior corneal surface, and $x = L$ specifies the posterior cornea/anterior chamber interface. Oxygen concentration at the electrode surface is zero because of the limiting-current condition.[67] Reaction 1 consumes oxygen completely at the cathode surface, thereby drawing oxygen toward that surface. Thus, there is always a net flux of oxygen in the membrane directed toward the electrode surface. This is illustrated in Figure 1 by the positive slope of all tension profiles at $x = -L_m$. This observation contrasts with that of Fatt and colleagues[39–41] who argued that oxygen initially in the membrane supplies the cornea with negligible loss to the electrode. Figure 2 contrasts the concentration profiles in the interpretation scheme of Fatt and colleagues, where the oxygen tension in the membrane falls uniformly as oxygen is supplied from the membrane to the cornea but not to the electrode.

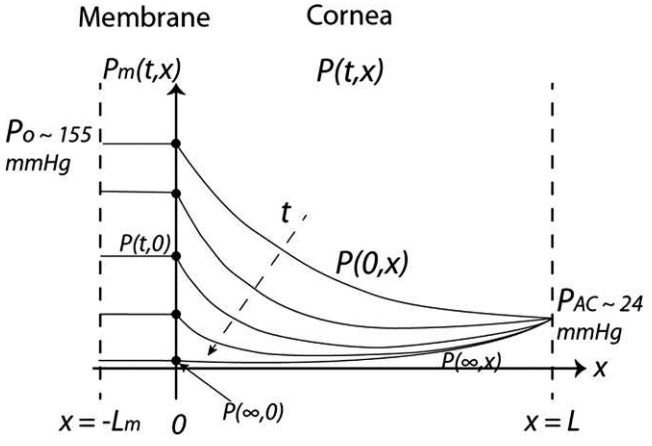

Figure 2. Schematic of oxygen partial-pressure profiles upon placing the microelectrode onto the cornea according to Fatt and colleagues.[39–41] The spatially uniform tension profiles in the membrane are incorrect (compare with Fig. 1).

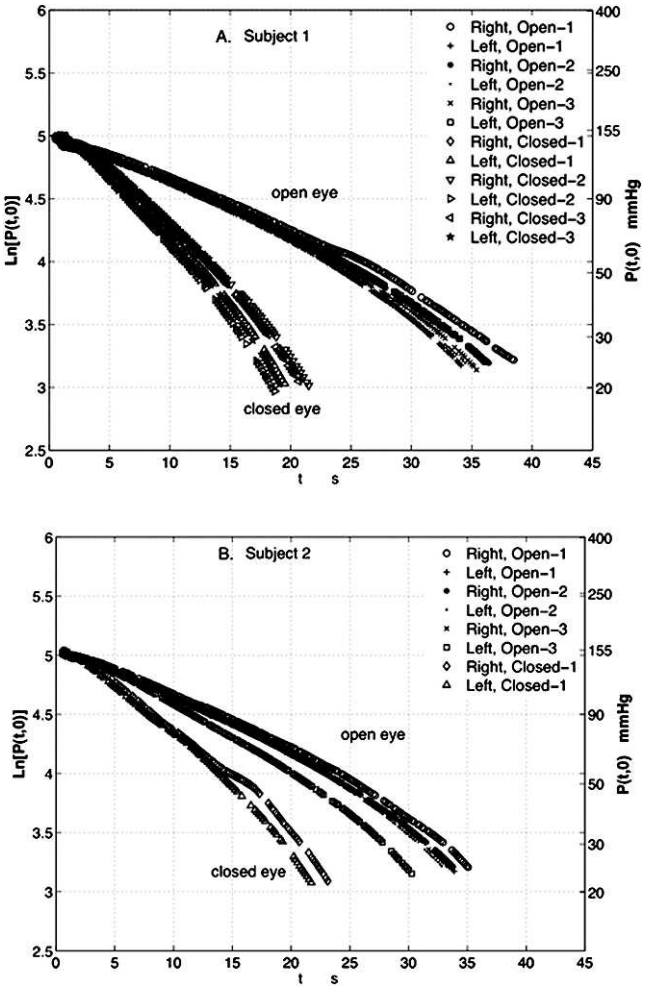

Figure 3. Measured open- and closed-eye oxygen partial pressures reported as a semilogarithmic graph of $ln[P(t,0)]$ and $P(t,0)$ versus time by the Clark-type polarographic electrode. (**A**) Repeat trials for Subject 1. (**B**) Repeat trials for Subject 2. Oxygen tension is reported in mm Hg.

Dashed profiles in Figure 1 correspond to very early time when the flux to the cathode is high. In this time period, the polarographic-oxygen-sensor (POS) signal does not correspond to the oxygen tension at the membrane/epithelial interface because the tension profile in the membrane is not linear, corresponding to that established during calibration. For times exceeding L^2_m/D_m, where D_m is the diffusivity of oxygen in the membrane, membrane tension profiles approach linearity corresponding to a pseudosteady state, as shown by the solid lines in Figure 1. Once the profiles in the membrane become linear, the POS correctly reflects the oxygen tension at the epithelium/membrane surface, shown as filled circles in Figure 1 at $x = 0$. For a polymer membrane with an oxygen diffusivity of 2×10^{-7} cm^2/s,[68–70] concentration profiles adjust to a pseudosteady state in less than L^2_m/D_m, or approximately 5 seconds for a 10-μm thick membrane and 20 seconds for a 20-μm thick membrane. Typical microelectrode measurements occur over time

frames of approximately 30 seconds (see Fig. 3). In the time frame beyond L^2_m/D_m, the membrane is well approximated by the pseudosteady form of Fick's second law at each time step. Thus, beyond 5 to 20 seconds, depending on membrane material and thickness, oxygen-tension profiles in the membrane, $P_m(t,x)$, are linear starting from the membrane initially saturated at environmental oxygen tension (155 mm Hg). Once at pseudosteady state, the net flux of oxygen through the membrane is toward the microelectrode and is supplied by the cornea (see Fig. 1).

As shown in Figure 1, for times very soon after establishment of membrane pseudosteady state, oxygen flux at the epithelium (i.e., at $x = 0$) is directed into the cornea (i.e., a negative slope for the profile $P[0,x]$). Just beyond $x = 0$, the transient epithelial flux soon reverses direction to meet the demand of the microelectrode to maintain zero oxygen concentration at $x = -L_m$. Accordingly, a maximum tension appears in the corneal tension profile near $x = 0$. Farther into the cornea, oxygen diffuses inward diminishing in concentration due to metabolic loss. Oxygen is also supplied for corneal metabolic need by the anterior chamber. This flux remains directed into the cornea during on-eye placement of the microelectrode. Thus, the slope of the tension profile remains positive at $x = L$. The maximum in the cornea-tension profiles moves inward in time, eventually merging into a monotonic decline directed from the anterior chamber to the epithelium. Finally, a final steady-state profile, labeled as $P(\infty,x)$ in Figure 1, is reached where oxygen supply from the anterior chamber matches that demanded by the microelectrode and by the cornea.

We desire $J_o(0)$, the flux of oxygen into the anterior cornea at zero time corresponding to that established before the microelectrode was emplaced. $J_o(0)$ is also referred to as the oxygen uptake into the anterior cornea and is typically reported in volumetric units of μL O_2(STP)/cm^2/h. As noted above, oxygen is also supplied to the cornea from the anterior chamber. However, during open eye, the amount of oxygen supplied by the anterior chamber is negligible.[1–3,71] Likewise, for the closed eye, a majority of the oxygen supply before POS emplacement is from the palpebral conjunctiva.[1–3,71] In both open and closed eye, $J_o(0)$ reflects oxygen supply to the epithelium and to a portion of the anterior stroma. Since the oxygen-tension profiles in the membrane are linear, the measured limiting current is directly proportional to $P(t,0)$. Thus, our goal is to relate $P(t,0)$ to the initial oxygen flux into the cornea at $x = 0$.

Filled circles in Figure 1 illustrate qualitatively how the measured polarographic oxygen tension falls in time starting from $P_o = 155$ mm Hg (open eye) down to the steady state of $P(\infty,0)$. The value of $P(\infty,0)$ is much less than 24 mm Hg, the oxygen tension in the anterior chamber. A reactive-diffusion model is required to convert the measured transient decline of $P(t,0)$ to oxygen uptake. A brief summary of that model is outlined below. Full model development is summarized in Appendices A and B (see Supplementary Material and Supplementary Appendices A and B, http://www.iovs.org/lookup/suppl/doi:10.1167/iovs.12-10059/-/DCSupplemental).

Reactive-Diffusion Model

From Figure 1, diffusion of oxygen through the cornea and the covering membrane must be described. For the protective membrane where there is no oxygen reaction, application of Fick's second law in the pseudo-steady state gives the result

$$P_m(t,x) = P(t,0)(1 + x/L_m) \tag{2}$$

where P_m is the local oxygen partial pressure in the membrane. Equation 2 describes a linear concentration profile with zero concentration at the electrode surface (i.e., at $x = -L_m$). A linearly declining oxygen concentration profile from the epithelium to the cathode diagnoses oxygen flux into the electrode. Again, Equation 2 holds only in a pseudosteady membrane or for times longer than $D_m t/L^2_m > 1$.

Table 1. Parameters

Parameter (units)	Value	Source
D_m (cm^2/s)*	2.44×10^{-7}	Jensen et al.[68] and Kroschwitz et al.[69]
D (cm^2/s)†	1.28×10^{-5}	Chhabra et al.[1]
k_m (mL[STP]/[mL mm Hg])	6.97×10^{-5}	Jauregui and Fatt[40]
k (mL[STP]/[mL mm Hg])	2.30×10^{-5}	Chhabra et al.[71]
L_m (μm)	18	–
L (μm)	480	Chhabra et al.[1]
$\beta = DkL_m/(D_m k_m L)$	0.649	–
b_1	2.18	–

* Determined from measured oxygen permeability in the polymer membrane ($D_m k_m = 1.7$ Barrer[68,69]) after division by the partition coefficient $k_m = 6.97 \times 10^{-5}$ mL[STP]/[mL mm Hg]).[40]

† Determined from oxygen permeability in the stroma ($Dk = 29.5$ Barrer[1] after division by the partition coefficient $k = 2.3 \times 10^{-5}$ mL(STP)/(mL mm Hg).[71]

For the cornea, conservation of oxygen species requires that[71]

$$k\frac{\partial P(t,x)}{\partial t} = Dk\frac{\partial^2 P(t,x)}{\partial x^2} - Q(P) \tag{3}$$

where k is the partition coefficient of oxygen in the cornea, D is the diffusivity of oxygen in the cornea, and Q is the local rate of oxygen metabolic loss. In the present analysis, we averaged over the three layers of the cornea. Boundary conditions for equation 3 are that the partial pressure of oxygen at the endothelium/anterior-chamber interface is fixed, $P(t,L) = P_{AC}$ (24 mm Hg), and that at the membrane/anterior-cornea interface is $P(t,0)$. We follow Chhabra et al.[1,71] and adopt Monod kinetics for oxygen consumption:

$$Q = Q_{\max}P/(K + P) \tag{4}$$

where Q_{max} is the maximum consumption rate, and K is the Monod constant or the value of oxygen partial pressure when the reaction rate is one-half maximum. Nonlinearity of the rate expression in Equation 4 demands a numerical solution to the problem. Here, we adopt a simple limiting form for use in Equation 4 valid at low partial pressure where the consumption rate depends linearly on oxygen concentration

$$Q = (Q_{\max}/K)P = k_1 P \text{ for } P/K \ll 1 \tag{5}$$

where $k_1 \equiv Q_{max}/K$ is the first-order rate constant or the zero-tension slope of the Monod rate expression. Imposition of a pseudosteady state requires tension data at longer times where $P(t,0)$ is close to and possibly below that of the anterior chamber (see Fig. 1). At these low tensions, Equation 5 is a useful approximation.

The solution to Equation 3 also requires an initial condition. In the micropolarographic experiment, the cornea is initially at a steady state with a fixed anterior partial pressure, P_o. For open eye, this value is 155 mm Hg, whereas for closed eye, it is 61.5 mm Hg.[1–3,71] The steady form of Equation 3 is

$$0 = Dk\frac{d^2 P(0,x)}{dx^2} - k_1 P(0,x) \tag{6}$$

Boundary conditions are $P(0,0) = P_o$ and $P(0,L) = P_{AC}$. Equation 6 is solved in Equation A1 of Appendix A (see Supplementary Material and Supplementary Eq. A1, http://www.iovs.org/lookup/suppl/doi:10.1167/iovs.12-10059/-/DCSupplemental) to give $P(0,x)$ that, in turn, serves as the initial condition for Equation 3. As discussed in Appendix A (see Supplementary Material and Supplementary Appendix A, http://www.iovs.org/lookup/suppl/doi:10.1167/iovs.12-10059/-/DCSupplemental), Equations 2, 3, 5, and 6 admit analytic solution by Laplace transform[72,73] to quantify the desired unsteady oxygen partial pressure profile in the cornea, $P(t,x)$.

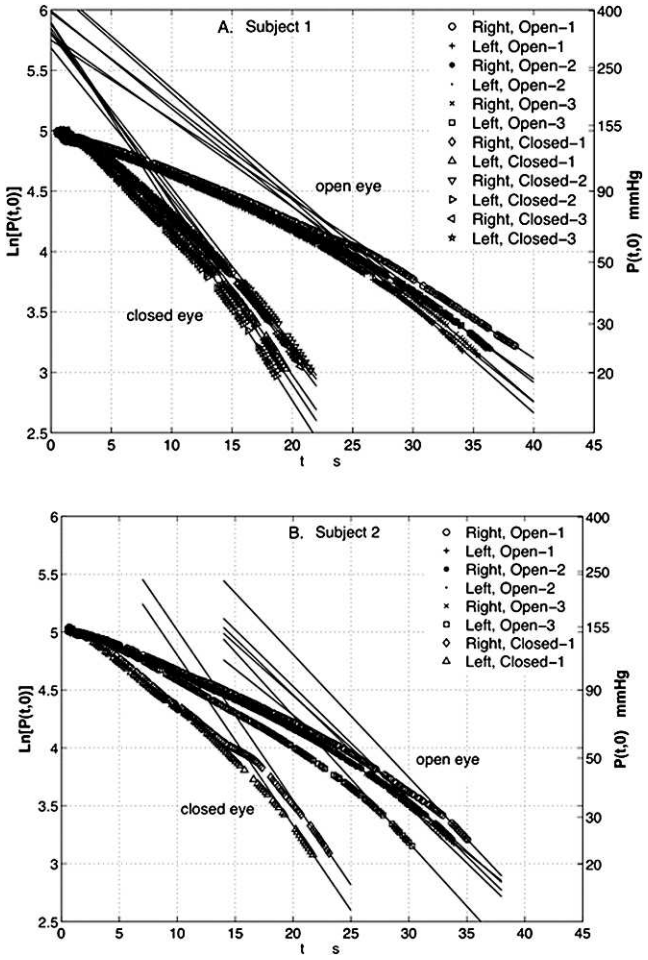

Figure 4. Measured open- and closed-eye oxygen partial pressures from Figure 3 reported as a semilogarithmic graph of $ln[P(t,0)]$ and $P(t,0)$ versus time by the Clark-type polarographic electrode. (**A**) Repeat trials for Subject 1. (**B**) Repeat trials for Subject 2. Oxygen tension is reported in mm Hg. *Least-squares-fit lines* are drawn through the semilogarithmic linear regions of the experimental data.

We seek the oxygen flux, $J_o(0)$, corresponding to the initial tension profile described by the solution of Equation 6 (i.e., the steady-state oxygen uptake before placement of the POS). Appendix A (see Supplementary Material and Supplementary Appendix A, http://www.iovs.org/lookup/suppl/doi:10.1167/iovs.12-10059/-/DCSupplemental) demonstrates that

$$J_o(0) = \varphi\left[\frac{\cosh\varphi - P_{AC}/P_o}{\sinh\varphi}\right]Dk\frac{P_o}{L} \qquad (7)$$

where $\varphi \equiv \sqrt{k_1L^2/Dk}$ is the Thiele modulus.[74] Calculation of $J_o(0)$ from Equation 7 thus requires knowledge of the average oxygen permeability of the cornea, Dk, the corneal thickness, and the first-order metabolic consumption rate constant, k_1 (embedded in the Thiele modulus). Appendix A (see Supplementary Material and Supplementary Appendix A, http://www.iovs.org/lookup/suppl/doi:10.1167/iovs.12-10059/-/DCSupplemental) reveals that the values for the oxygen diffusion and partition coefficients of the membrane, D_m and k_m, respectively, are also needed in the analysis. Table 1 lists the chosen parameter values and their sources. D and k are approximated as those of the stroma and are taken from Chhabra et al.[1–3,71] To obtain k_1, oxygen-tension data from the Clark electrode must be analyzed as described below.

Experiment

A Clark-type polarographic oxygen sensor (Radiometer E5047/0 and Radiometer Amplifier PHM 73; Radiometer, Copenhagen, Denmark) linked to a personal computer was used to assess the corneal oxygen uptake rate of each subject. The supplied probe was equipped with a 30-μm diameter platinum cathode and 18-μm thick polypropylene membranes. To convert the probe limiting current to oxygen tension, the POS was calibrated in purified water (Milli-Q; Millipore Corp., Billerica, MA) at 36°C saturated with air (155 mm Hg O_2) and with pure nitrogen (0 mm Hg O_2), respectively. Probe calibration was routinely checked by immersion in the nitrogen-saturated aqueous solution. For all oxygen-uptake measurements, the POS protective membrane was saturated initially with oxygen at 155 mm Hg.

Ten nonhabitual contact lens wearers were enrolled in a prospective, nondispensing, randomized, open-label clinical study. The study was approved by the local Ethics Committee and was conducted in accordance with the Declaration of Helsinki. Transient corneal oxygen-tension was measured in both eyes of every subject: three times under open-eye condition and one time after 5 minutes of eye closure. During open-eye measurements, subjects fixated straight ahead at a target 3 m away, and the POS was applied perpendicularly onto the center of the cornea. For the closed-eye condition, subjects kept their head erect, and the POS was applied immediately on the center of the cornea after eye opening while the contralateral eye was fixated on the distant target. Measured oxygen-tension decline curves were analyzed as described below to ascertain corneal oxygen uptake rate. Figure 3 illustrates typical tension-decline histories for two subjects.

Analysis of Polarographic Data

A properly calibrated POS operating in the pseudosteady state detects partial pressure of oxygen at the covering membrane/anterior cornea interface, or $P(t,0)$ in Figures 1 and 3. To establish oxygen uptake, the measured transient oxygen tension must first be analyzed to obtain the unknown rate constant k_1. Appendix A (see Supplementary Material and Supplementary Appendix A, http://www.iovs.org/lookup/suppl/doi:10.1167/iovs.12-10059/-/DCSupplemental) demonstrates that

$$P(t,0) = P(\infty,0) + \sum_{n=1}^{\infty} A_n \exp(-\alpha_n t) \qquad (8)$$

where $P(\infty,0)$ is the final steady oxygen partial pressure at the membrane/anterior cornea interface, and constants α_n and A_n are given by Equations A16 and A17 in Appendix A (see Supplementary Material and Supplementary Equations A16 and A17, http://www.iovs.org/lookup/suppl/doi:10.1167/iovs.12-10059/-/DCSupplemental). In addition to a dependence on the running index, n, the constants α_n and A_n contain the desired rate constant k_1 for use in Equation 7. Note in Equation 8 that the measured microelectrode partial pressures at early time do not decay as a single exponential.[39–41] Rather, we find a series of exponential decays. The experimental data in Figure 3 confirm nonlinear behavior at an early time on a semilogarithmic scale.

Inspection of Figure 3 demonstrates that semilogarithmic linear behavior emerges only at a later time. Therefore, to obtain the corneal oxygen-consumption rate constant, we evaluate Equation 8 at later time, where the measured partial pressure approaches the final steady state

$$P(t,0) = P(\infty,0) + A_1\exp(-\alpha_1 t) \qquad (9)$$

α_1^{-1} in Equation 9 is the longest time constant in Equation 8 and, therefore, controls long-time behavior. Appendix A (see Supplementary Material and Supplementary Appendix A, http://www.iovs.org/lookup/suppl/doi:10.1167/iovs.12-10059/-/DCSupplemental) demon-

Table 2. Open-Eye Oxygen Uptake*

Subject	α_1, s^{-1}	k_1k^{-1}, s^{-1}	$J_o(0)$, μL/(cm² h) This Work†	$J_o(0)$, μL/(cm² h) Fatt Procedure[40]
1	0.0782 ± 0.0091	0.0517 ± 0.0091	10.3 ± 0.941	2.94 ± 0.128
2	0.0966 ± 0.0116	0.0701 ± 0.0116	12.0 ± 1.04	3.38 ± 0.312
3	0.0913 ± 0.0107	0.0647 ± 0.0107	11.6 ± 0.995	3.26 ± 0.253
4	0.0896 ± 0.0282	0.0631 ± 0.0282	11.2 ± 2.92	2.88 ± 0.584
5	0.0851 ± 0.0141	0.0586 ± 0.0141	11.0 ± 1.28	3.00 ± 0.232
6	0.0935 ± 0.0056	0.0670 ± 0.0056	11.8 ± 0.500	3.34 ± 0.246
7	0.115 ± 0.0082	0.0888 ± 0.0082	13.6 ± 0.647	3.28 ± 0.0753
8	0.0772 ± 0.0095	0.0507 ± 0.0095	10.2 ± 1.01	3.03 ± 0.257
9	0.0673 ± 0.0125	0.0408 ± 0.0125	9.09 ± 1.43	2.94 ± 0.175
10	0.102 ± 0.0031	0.0754 ± 0.0031	12.5 ± 0.263	3.36 ± 0.137

* All error estimates are based on 95% confidence in a Student's *t*-test.
† Calculated from Equation 7 using $P_o = 155$ mm Hg.

strates that $P(\infty,0)/P(t,0) < 1$ so $P(\infty,0)$ can safely be neglected in Equation 9 or

$$ln\ P(t,0) = ln\ A_1 - \alpha_1 t \qquad (10)$$

This result indicates that at long times, a semilogarithmic graph of the polarographic-measured partial pressure versus time yields a straight line with negative slope α_1. Figure 4 confirms this assertion and illustrates typical best eye-fit straight lines whose slopes give α_1 for each repeat experiment. Given the experimentally determined value of α_1, the metabolism rate constant is available in Appendix A (see Eq. A16 for $n = 1$; see Supplementary Material and Supplementary Appendix A and Eq. A16, http://www.iovs.org/lookup/suppl/doi:10.1167/iovs.12-10059/-/DCSupplemental)

$$\varphi^2 \equiv k_1L^2/Dk = L^2\alpha_1/D - b_1^2 \qquad (11)$$

where b_1 is established by trial-and-error from (see Eq. A15 for $n = 1$; see Supplementary Material and Supplementary Eq. A15, http://www.iovs.org/lookup/suppl/doi:10.1167/iovs.12-10059/-/DCSupplemental)

$$\tan b_1 + \beta b_1 = 0 \qquad (12)$$

where $\beta = DkL_m/(D_mk_mL)$ is the ratio of diffusion resistance in the membrane to that in the cornea. Hence, to establish the metabolic rate constant, the diffusive properties of both the cornea and the probe membrane must be known. In Table 1, we adopt an average value of D and k characteristic of the stroma[1–3,71] and reported literature values for D_m and k_m.[40,68–70] Resulting values for β and b_1 are also listed in Table 1. Different polarographic probes may be fitted with differing membrane materials and with differing thicknesses, so β must be determined for each instrument. Once φ and b_1 are calculated from Equations 11 and 12, oxygen uptake follows from Equation 7. Thus, from the measured linear semilogarithmic slope of the tension decline at later times, α_1, oxygen uptake follows from application of Equations 7, 11, and 12.

It is possible to estimate $J_o(0)$ from the intercept of the linear semilogarithmic slope in Equation 10 through the value of A_1. We find, however, that values of A_1 so obtained are large and scattered. Appendix A (see Supplementary Material and Supplementary Appendix A, http://www.iovs.org/lookup/suppl/doi:10.1167/iovs.12-10059/-/DCSupplemental) confirms that calculation of $J_o(0)$ from A_1 is imprecise.

Results

Figure 4 indicates best eye-fit straight lines corresponding to the late-time, linear semilogarithmic behavior predicted by Equation 10 for two human subjects. Each repeat experiment displays a somewhat different slope indicating reproducibility for the different repeated trials. Table 2 summarizes our results for 10 subjects averaged over repeat measurements on the left and right eyes for open-eye conditions. Reported in Table 2 are the average values of α_1 and corresponding error limits at 95% confidence, along with the calculated rate constant, expressed as k_1/k, and the oxygen uptake, $J_o(0)$ in μL O_2(STP)/cm²/h calculated from α_1 and Equations 7, 11, and 12. Deviations for $J_o(0)$ reflect the 95% confidence deviations in the measured slopes α_1. Although closed-eye POS data were successfully analyzed to obtain α_1 values (see straight lines for closed eye in Fig. 4), we do not report oxygen-uptake results for the closed eye in Table 2 because a membrane pseudosteady state is likely not obeyed within 20 seconds. Thus, closed-eye results may not be quantitatively reliable.

The last column in Table 2 reports oxygen uptake ascertained from our micropolarography measurements following the classical procedure where oxygen uptake is calculated according to the well-mixed membrane model[40]

$$J_o(0) = k_mL_m[-dP(0)/dt] \qquad (13)$$

Although various methods are used to estimate $dP(0)/dt$ in Equation 13,[48] we adopt the specific recommendation of Jauregui and Fatt.[40] In the semilogarithmic graph of measured tension versus time, as in Figure 3, a straight line corresponding to the initial slope is drawn to a value of tension 90% lower than the initial value (i.e., $P_o = 155$ mm Hg for open eye or 61.5 mm Hg for closed eye) to give the time, t_1. $dP(0)/dt$ is then calculated as $0.1(P_o/t_1)$. This procedure clearly gives a lower characteristic slope in Figure 3 than that corresponding to α_1, and accordingly yields smaller oxygen uptake values.

Anterior oxygen uptake for the 10 subjects studied is around 11 μL(STP)/(cm² h) at open eye. The calculation procedure of Fatt and colleagues for the same subjects gives uptake values three to five times smaller. Variability among the limited number of subjects is not large for both analysis procedures. Though not quantitatively precise, our closed-eye uptake values are around 6 μL(STP)/(cm² h). Closed-eye uptake in the protocol of Fatt and colleagues is also consistently lower than those of open eye by a factor of approximately two.

Discussion

Available micropolarographic oxygen-uptake values for the open-eye human cornea display a wide range over subjects and laboratories ranging from 1 to 10 μL(STP)/(cm² h),[40,48,52,55,75] with an average of approximately 5 μL(STP)/(cm² h).[48] Our results agree with the higher reported values and do not exhibit strong variability among subjects. Our sample size, however, is not large. We stress that all literature uptake values are based on the invalid interpretation scheme of Fatt and colleagues.[39–41] Equation 13

assumes that the membrane is well mixed and supplies oxygen to the cornea. These assumptions are invalid because the Clark electrode measures electrical current corresponding to oxygen reduction at the cathode (compare Figs. 1, 2). Furthermore, initial oxygen-tension data do not follow a single-exponential transient decay, so evaluation of the derivative in Equation 13 is ambiguous. We assert that the reason for our observed larger uptake values is that the classical analysis procedure[39–41] is suspect.

We are unable to present reliable oxygen uptake for closed eye for two reasons. First, the membrane thickness is too large (ca. 20 μm) to achieve pseudosteady state within the 20-second time interval of the POS experiment. We strongly recommend the use of thin, high-oxygen-permeability membrane probe covers. For example, replacing the 20-μm thick membrane with a 10-μm thick membrane allows a pseudosteady state in approximately 5 seconds in Figure 3. In this case, assessment of uptake from the closed-eye data would be quantitative. Only when the membrane achieves a pseudosteady state is the measured electrical current linearly related to oxygen tension. Similarly, we recommend use of cathode radii that are several times larger than the thickness of the covering membrane so that a one-dimensional analysis applies quantitatively.[68]

Second, our closed-eye experiments do not conform exactly to the proposed theory. The protective membrane is initially saturated at 155 mm Hg. Thus, at the early time in the closed-eye experiment, our model strictly does not apply because it assumes an initial tension in the membrane of 61.5 mm Hg, that of the palpebral conjunctiva. This means that the time necessary to establish a pseudosteady state in the membrane is longer since the membrane oxygen tension must fall from 155 mm Hg to those characteristic of the closed eye. Future research should saturate the protective membrane at a tension as near as possible to the epithelial tension existing before probe placement.

Acknowledgments

P. Lazon de la Jara, B. Holden, K. Ehrmann, and A. Ho thank the Australian Government Cooperative Research Centre Program and the Brien Holden Vision Institute for financial support in conducting the experiments.

References

1. Chhabra M, Prausnitz JM, Radke CJ. Modeling corneal metabolism and oxygen transport during contact lens wear. *Optom Vis Sci*. 2009;86:454–466.
2. Leung BK, Bonanno JA, Radke CJ. Oxygen-deficient metabolism and corneal edema. *Prog Retin Eye Res*. 2011;30:471–492.
3. Takatori SC, Radke CJ. A quasi-2-dimensional model for respiration of the cornea with soft contact lens wear. *Cornea*. 2012;31:405–417.
4. Bruce AS, Brennan NA. Corneal pathophysiology with contact lens wear. *Surv Ophthalmol*. 1990;35:25–58.
5. Smelser GK, Chen DK. Physiological changes in cornea induced by contact lenses. *AMA Arch Ophthalmol*. 1955;53:676–679.
6. Sweeney DF. Clinical signs of hypoxia with high-Dk soft lens extended wear: is the cornea convinced? *Eye Contact Lens*. 2003;29(suppl 1):S22–S25; discussion S26–S29, S192–S194.
7. Hill RM, Fatt I. Oxygen deprivation of the cornea by contact lenses and lid closure. *Am J Optom Arch Am Acad Optom*. 1964;41:678–687.
8. Huang P, Zwang-Weissman J, Weissman BA. Is contact lens "T" still important? *Cont Lens Anterior Eye*. 2004;27:9–14.
9. Hill RM, Fatt I. Oxygen measurements under a contact lens. *Am J Optom Arch Am Acad Optom*. 1964;41:382–387.
10. Brennan NA. Beyond flux: total corneal oxygen consumption as an index of corneal oxygenation during contact lens wear. *Optom Vis Sci*. 2005;82:467–472.
11. Efron N, Brennan NA. In search of the critical oxygen requirement of the cornea. *Contax*. 1987;2:5–11.
12. Brennan NA, Efron N, Weissman BA, Harris MG. Clinical application of the oxygen transmissibility of powered contact lenses. *CLAO J*. 1991;17:169–172.
13. Holden BA, Mertz GW. Critical oxygen levels to avoid corneal edema for daily and extended wear contact lenses. *Invest Ophthalmol Vis Sci*. 1984;25:1161–1167.
14. Fatt I, Neumann S. The average oxygen transmissibility of contact lenses: application of the concept to laboratory measurements, clinical performance and marketing. *Contact Lens J*. 1990;18:80–85.
15. Fatt I, Ruben CM. A new oxygen transmissibility concept for hydrogel contact lenses. *J Br Contact Lens Assoc*. 1993;16:141–149.
16. Fatt I, Ruben CM. The point-to-point variation of oxygen delivery to a cornea covered by a hydrogel contact lens in the open eye. *Int Contact Lens Clin*. 1994;21:50–56.
17. Morgan PB, Efron N. The oxygen performance of contemporary hydrogel contact lenses. *Cont Lens Anterior Eye*. 1998;21:3–6.
18. O'Neal MR, Polse KA, Fatt I. Oxygen permeability of selected GPH polymers and predictions of tear layer oxygen tension. *Int Contact Lens Clin*. 1983;10:256–266.
19. Efron N, Fitzgerald JP. Distribution of oxygen across the surface of the human cornea during soft contact lens wear. *Optom Vis Sci*. 1996;73:659–665.
20. Fatt I. Is there a problem in EOP land? *Int Contact Lens Clin*. 1993;20:150–152.
21. Fatt I. Have we found the cornea's "critical oxygen requirement"? *Optician*. 1987;194:17–21.
22. Fatt I. New physiological paradigms to assess the effect of lens oxygen transmissibility on corneal health. *CLAO J*. 1996;22:25–29.
23. Compan V, Lopez-Alemany A, Riande E, Refojo MF. Biological oxygen apparent transmissibility of hydrogel contact lenses with and without organosilicon moieties. *Biomaterials*. 2004;25:359–365.
24. Weissman BA, Fazio DT. Human corneal oxygen flux under soft contact lenses. *Am J Optom Physiol Opt*. 1982;59:635–638.
25. Polse KA, Mandell RB. Critical oxygen tension at the corneal surface. *Arch Ophthalmol*. 1970;84:505–508.
26. Mandell RB, Polse KA, Fatt I. Corneal swelling caused by contact lens wear. *Arch Ophthalmol*. 1970;83:3–9.
27. Harvitt DM, Bonanno JA. Re-evaluation of the oxygen diffusion model for predicting minimum contact lens Dk/t values needed to avoid corneal anoxia. *Optom Vis Sci*. 1999;76:712–719.
28. Hill RM, Fatt I. Oxygen uptake from a reservoir of limited volume by the human cornea in vivo. *Science*. 1963;142:1295–1297.
29. Hill RM, Fatt I. Oxygen depletion of a limited reservoir by human conjunctiva. *Nature*. 1963;200:1011–1012.
30. Bonanno JA, Stickel T, Nguyen T, et al. Estimation of human corneal oxygen consumption by noninvasive measurement of tear oxygen tension while wearing hydrogel lenses. *Invest Ophthalmol Vis Sci*. 2002;43:371–376.
31. Harvitt DM, Bonanno JA. Direct noninvasive measurement of tear oxygen tension beneath gas-permeable contact lenses in rabbits. *Invest Ophthalmol Vis Sci*. 1996;37:1026–1036.

32. Brennan NA. Corneal oxygenation during contact lens wear: comparison of diffusion and EOP-based flux models. *Clin Exp Optom*. 2005;88:103–108.
33. Alvord LA, Hall WJ, Keyes LD, Morgan CF, Winterton LC. Corneal oxygen distribution with contact lens wear. *Cornea*. 2007;26:654–664.
34. Fatt I. Steady-state distribution of oxygen and carbon dioxide in the in vivo cornea. II. The open eye in nitrogen and the covered eye. *Exp Eye Res*. 1968;7:413–430.
35. Fatt I, Bieber MT. The steady-state distribution of oxygen and carbon dioxide in the in vivo cornea. I. The open eye in air and the closed eye. *Exp Eye Res*. 1968;7:103–112.
36. Fatt I, Bieber MT, Pye SD. Steady state distribution of oxygen and carbon dioxide in the in vivo cornea of an eye covered by a gas-permeable contact lens. *Am J Optom Arch Am Acad Optom*. 1969;46:3–14.
37. Fatt I, Freeman RD, Lin D. Oxygen tension distributions in the cornea: a re-examination. *Exp Eye Res*. 1974;18:357–365.
38. Fatt I, Lin D. Spatial distribution of oxygen in the cornea of a closed eye wearing a gas permeable contact lens. *Curr Eye Res*. 1985;4:723–724.
39. Fatt I. Measurement of oxygen flux into the cornea by pressing a sensor onto a soft contact lens on the eye. *Am J Optom Physiol Opt*. 1978;55:294–301.
40. Jauregui MJ, Fatt I. Estimation of oxygen tension under a contact lens. *Am J Optom Arch Am Acad Optom*. 1971;48: 210–218.
41. Rasson JE, Fatt I. Oxygen flux through a soft contact lens on the eye. *Am J Optom Physiol Opt*. 1982;59:203–212.
42. Clark LC Jr, Sachs G. Bioelectrodes for tissue metabolism. *Ann N Y Acad Sci*. 1968;148:133–153.
43. Clark LC Jr, Wolf R, Granger D, Taylor Z. Continuous recording of blood oxygen tensions by polarography. *J Appl Physiol*. 1953;6:189–193.
44. Farris RL, Takahashi GH, Donn A. Oxygen flux across the in vivo rabbit cornea. *Arch Ophthalmol*. 1965;74:679–682.
45. Fatt I. An ultramicro oxygen electrode. *J Appl Physiol*. 1964; 19:326–329.
46. Fatt I. The oxygen electrode: some special applications. *Ann N Y Acad Sci*. 1968;148:81–92.
47. Fatt I, Helen RS. A multicathode polarographic oxygen sensor and its performance. *J Appl Physiol*. 1969;27:435–437.
48. Fink B, Hill RM. Corneal oxygen uptake: a review of polarographic techniques, applications, and variables. *Cont Lens Anterior Eye*. 2006;29:221–229.
49. Fink BA, Carney LG, Hill RM. Intra-subject variability of human corneal oxygen uptake. *Int Contact Lens Clin*. 1990;17:224–227.
50. Fitzgerald JP, Efron N. Oxygen uptake profile of the human cornea. *Clin Exp Optom*. 1986;69:149–152.
51. Larke JR, Parrish ST, Wigham CG. Oxygen sensors for clinical use. *Cont Lens Anterior Eye*. 1980;3:70–74.
52. Larke JR, Parrish ST, Wigham CG. Apparent human corneal oxygen uptake rate. *Am J Optom Physiol Opt*. 1981;58:803–805.
53. Lazon de la Jara P, Holden BA, Terry R, La Hood D, Ehrmann K. Oxygen levels and oxygen flux with silicone hydrogel contact lenses under open and closed eye conditions. Poster presented at: the American Academy of Optometry (AAO) meeting; December 7–9, 2006; Denver, CO.
54. Parrish ST, Larke JR. Apparent corneal oxygen uptake rate and debt in contact lens wearing subjects. *Cont Lens Anterior Eye*. 1982;5:54–58.
55. Quinn TG, Schoessler JP. Human corneal epithelial oxygen demand–population characteristics. *Am J Optom Physiol Opt*. 1984;61:386–388.
56. Takahashi GH, Fatt I. The diffusion of oxygen in the cornea. *Exp Eye Res*. 1965;4:4–12.
57. Takahashi GH, Fatt I, Goldstick TK. Oxygen consumption rate of tissue measured by a micropolarographic method. *J Gen Physiol*. 1966;50:317–335.
58. Augsburger AR, Hill RM. Corneal anesthetics and epithelial oxygen flux. *Arch Ophthalmol*. 1972;88:305–307.
59. Bentley CR, Larke JR. Apparent respiration rate of the human corneal epithelium with tetracaine HCl and benoxinate HCl. *Am J Optom Physiol Opt*. 1983;60:960–963.
60. Chi JM, Fink BA, Hill RM, Mitchell GL. Factors influencing the measurement of oxygen shortfall of the human cornea: sequencing of test conditions. *Cont Lens Anterior Eye*. 2007;30:17–21.
61. Holden BA, Polse KA, Fonn D, Mertz GW. Effects of cataract surgery on corneal function. *Invest Ophthalmol Vis Sci*. 1982; 22:343–350.
62. Holden BA, Sweeney DF, Vannas A, Nilsson KT, Efron N. Effects of long-term extended contact lens wear on the human cornea. *Invest Ophthalmol Vis Sci*. 1985;26:1489–1501.
63. Morris J, Ruben M. Clinical aspects of the measurement of oxygen flux into the cornea. *Br J Ophthalmol*. 1981;65:97–100.
64. Newman JS, Thomas-Alyea KE. *Electrochemical Systems*. 3rd ed. Hoboken, NJ: John Wiley & Sons; 2004:377–405.
65. Chhabra M, Prausnitz JM, Radke CJ. A single-lens polarographic measurement of oxygen permeability (Dk) for hypertransmissible soft contact lenses. *Biomaterials*. 2007;28: 4331–4342.
66. Chhabra M, Prausnitz JM, Radke CJ. Polarographic method for measuring oxygen diffusivity and solubility in water-saturated polymer films: application to hypertransmissible soft contact lenses. *Ind Eng Chem Res*. 2008;47:3540–3550.
67. Mancy KH, Okun DA, Reilley CN. A galvanic cell oxygen analyzer. *J Electroanal Chem*. 1962;4:65–92.
68. Jensen OJ, Jacobsen T, Thomsen K. Membrane-covered oxygen electrodes: I. Electrode dimensions and electrode sensitivity. *J Electroanal Chem Interfacial Electrochem*. 1978;87:203–211.
69. Kroschwitz JI, Seidel A. *Kirk-Othmer Encyclopedia of Chemical Technology*. 5th ed. Hoboken, NJ: Wiley-Interscience; 2004:381–382.
70. van Krevelen DW, Nijenhuis K. Properties determining mass transfer in polymeric systems. In: van Krevelen DW, Nijenhuis K. *Properties of Polymers: Their Correlation with Chemical Structure, their Numerical Estimation and Prediction from Additive Group Contributions*. 3rd ed. Amsterdam, The Netherlands: Elsevier; 1990:544.
71. Chhabra M, Prausnitz JM, Radke CJ. Diffusion and Monod kinetics to determine in vivo human corneal oxygen-consumption rate during soft contact-lens wear. *J Biomed Mater Res B*. 2009;90B: 202–209.
72. Loney NW. Use of the residue theorem to invert Laplace transforms. *Chem Eng Educ*. 2001;35:22–24.
73. Wylie CR, Barrett LC. *Advanced Engineering Mathematics*. 5th ed. New York, NY: McGraw-Hill Book Company; 1982: 434–440.
74. Fogler H. Diffusion and reaction. In: Fogler HS. *Elements of Chemical Reaction Engineering*. 4th ed. Upper Saddle River, NJ: Prentice Hall; 2006:819–823.
75. Brennan NA. A model of oxygen flux through contact lenses. *Cornea*. 2001;20:104–108.